Chapter 4 Development of chemometric models to predict physical and chemical properties in biodiesel-diesel mixtures

Capítulo 4 Desarrollo de modelos quimiométricos para predecir propiedades físicas y químicas en mezclas biodiesel-diésel

RODRIGUEZ-PEREZ, Osniel Lázaro†*, ANGUEBES-FRANSESCHI, Francisco, ABATAL, Mohamed and MAY-TZUC, Oscar Jesús

Universidad Autónoma del Carmen, Campus III, Facultad de Ingeniería, Avenida Central S/N, Esq. con Fracc. Mundo Maya, C.P. 24115, Ciudad del Carmen, Campeche, México.

ID 1st Author: *Osniel Lázaro, Rodríguez-Pérez* / **ORC ID:** 0009-0000-7889-4508, **CVU CONAHCYT ID:** 1165367

ID 1st Co-author: *Francisco, Anguebes-Franseschi* / **ORC ID:** 0000-0002-5364-1165, **CVU CONAHCYT ID:** 217824

ID 2nd Co-author: *Mohamed, Abatal* / **ORC ID:** 0000-0003-2479-8769, **CVU CONAHCYT ID:** 203026

ID 3rd Co-author: *Oscar Jesús, May-Tzuc* / **ORC ID:** 0000-0001-7681-821, **CVU CONAHCYT ID:** 627799

DOI: 10.35429/H.2023.6.27.49

O. Rodríguez, F. Anguebes, M. Abatal, O. May

*fanguebes@pampano.unacar.mx

S. Vargas, S. Figueroa, C. Patiño and J. Sierra (AA. VV.) Engineering and Applied Sciences. Handbooks-TI-©ECORFAN-Mexico, Mexico City, 2023

Abstract

Renewable energies are necessary to cushion the warming of the earth; biodiesel can be used as a substitute for diesel, with the advantage that it is friendly to the environment. At present, the analyzes carried out on biodiesel by conventional methods are expensive and harmful to the environment. Therefore, the objective of this work is to build calibration models to predict properties of biodiesel and biodiesel-diesel mixtures based on Raman spectroscopy. The physical and chemical properties of biodiesel and blends were determined in accordance with ASTM D 6751 and EN 14214 standards, which were: free acidity index, flash point, density, specific gravity at 29.5 °C, °API density, weight specific, kinematic viscosity at 40°C and freezing point. For the construction of the models, the MATLAB numerical software was used together with its artificial neural network computational package. Model training was performed with 70% of the data, while the remaining 30% were used for testing and validation. The statistical criteria used for the accuracy of the chemometric models were the root mean square error (RMSE), mean absolute percentage error (MAPE) and the correlation coefficient (R^2). The results of the correlation coefficients between the real and predicted values obtained for each chemometric model were higher than 0.99%. The predictive capacity of the chemometric models was evaluated using the t-student test of paired data, where the t-student (tc) confidence values of each model were within the range of external validation (tv= ± 2.11). The results of the t-student demonstrate the predictive reliability of the models to determine the values of the physical and chemical properties carried out by the conventional methods indicated in the ASTM D6751 and EN 14214 standards.

Biodiesel, Diesel-biodiesel mixtures, Physicochemical properties, Raman spectroscopy and chemometric models

Resumen

Las energías renovables son necesarias para amortiguar el calentamiento de la tierra; el biodiesel puede emplearse como sustituto del diésel, con la ventaja que es amigable con el medio ambiente. En la actualidad los análisis realizados al biodiesel por métodos convencionales son costosos y perjudiciales con el medio ambiente. Por esto, el objetivo de este trabajo es construir modelos de calibración para predecir propiedades de biodiesel y mezclas de biodiesel-diésel fundamentado en la espectroscopia Raman. Las propiedades físicas y químicas del biodiesel y mezclas se determinaron conforme a las normas ASTM D 6751 y EN 14214, las cuales fueron: el índice de acidez libre, punto de inflamación, densidad, gravedad específica a 29.5 °C, densidad °API, peso específico, viscosidad cinemática a 40°C y punto de congelación. Para la construcción de los modelos se utilizó el software numérico MATLAB en conjunto de su paquete computacional de red neuronal artificial. El entrenamiento de los modelos se realizó con el 70 % de los datos, mientras que el 30 % restante se destinaron para las pruebas y validación. Los criterios estadísticos utilizados para la precisión de los modelos quimiométricos fueron el error cuadrático medio (RMSE), error de porcentaje absoluto medio (MAPE) y el coeficiente de correlación (R^2). Los resultados de los coeficientes de correlación entre los valores reales y predichos obtenidos para cada modelo quimiométrico fueron superiores al 0.99%. La capacidad de predicción de los modelos quimiométricos fue evaluada mediante la prueba *t-student* de datos apareados, donde los valores de confianza *t-student* (tc) de cada modelo estuvieron dentro del rango de validación externa (tv= ± 2.11). Los resultados del *t-student* demuestran la confiabilidad de predicción de los modelos para determinar los valores de las propiedades físicas y químicas realizadas por los métodos convencionales indicados en las normas ASTM D6751 y EN 14214.

Biodiesel, Mezclas diésel-biodiesel, Propiedades fisicoquímicas espectroscopia Raman y Modelos quimiométricos

1. Introduction

Currently, the main driver for the development of research on alternative energy sources is the urgent need to mitigate global warming and its consequences for living beings. For this, CO2 reduction is fundamental, since high concentrations of this greenhouse gas (GHG) are the main consequence of global warming [1]. However, the technologies that emit this type of gas are still economically unfeasible to eliminate. The power generation sector has a significant potential to reduce CO2 emissions, as it is responsible for almost 37.5 % of CO2 emissions worldwide [1].

A vital role can be played by renewable energy resources in reducing CO2 emissions. According to El-Sharkawy *et al*. [2] it is mentioned that if the share of renewable energy increases by 39 % by 2050 in combination with electricity generation, CO2 emissions can be reduced by up to 50 %. Currently, most of the world's energy demand is met by fossil fuels such as oil, coal and natural gas. Among the most consumed petroleum derivatives is diesel, which is widely used in transportation, agriculture, construction and power generation. However, the rapid rate of depletion of fossil oil, as well as environmental degradation due to vehicular and industrial pollution that directly affects the stable global ecosystem, has led to the search for new solutions to replace conventional diesel. Among the most viable alternatives to replace petrodiesel is biodiesel, which is a renewable fuel, biodegradable, non-toxic, does not alter the carbon cycle, has high lubricity and its characteristics are very similar to those of conventional diesel. This biofuel is a mixture of long-chain fatty acid esters (C14-C20), which is manufactured by the transesterification reaction of vegetable oils or animal fats with an alcohol in the presence of a catalyst. Also, its sulfur content is lower than the standard limit of conventional diesel, this being one of its main advantages, both for environmental care and for the life of combustion engines [3] [4]. Something very favorable is its miscibility with diesel, which allows blends of these two fuels in any proportion. Biomixes also emit less GHG when burned compared to conventional diesel [5]. Because of this, biodiesel production increased by 700% between 2005 and 2015 [6], reaching a global production of 48.3 billion liters in 2019 and demand in 2022 reached a record 170 billion liters, surpassing the levels observed in 2019 before the Covid-19 pandemic [7] [8].

The commercialization and use of biodiesel depend on its physicochemical properties, which are determined by specification limits depending on the type of regulation in the region being used. For example, standards have been established in the United States (ASTM D6751), Europe (EN 14214), Brazil, South Africa, Australia and other parts of the world. Both ASTM D6751 and EN 14214 efficiently detail biodiesel specifications, and these standards are commonly used as a reference or basis for other standards and their analyses. However, the conventional methods used to determine the physicochemical properties of biodiesel are slow and expensive, some are not accessible in some facilities, are environmentally destructive, and can cause human injury.

Therefore, this work is focused on determining in a different way the physicochemical properties of biodiesel, in a simple, non-destructive way and with a high level of accuracy. Consequently, chemometric models will be developed through artificial intelligence based on Raman spectroscopy, which have the priority of predicting properties such as: free acidity index, copper strip corrosion at 40 °C and 100 °C, sulfated ash content, flash point, density, specific gravity at 29.5 °C, density °API, specific weight, kinematic viscosity at 40°C and freezing point, complying with the established standards of ASTM D 6751 and EN 14214.

2. Materials and Methods

2.1 Materials

The materials used in this study were methanol (99.9% purity), phenolphthalein and sodium hydroxide (98.3%). The raw materials were chicken fat and pork fat. Chicken fat and skin were purchased from a chicken stand at a price of $5.00 MX per kilogram (kg) and washed thoroughly with tap water to remove debris such as blood, viscera, and bones. It was then cut into small pieces to be melted in a container at a temperature of 110ºC for 5 hours (h); the solid components of the lipid fraction of the fat (glycerides) were then separated in a fine mesh strainer. On the other hand, the pork fat used for the preparation of biodiesel was acquired through a butcher's shop at a price of $40.00 MX per kg. Then, it was heated in a DIDADEC TECHNOLOGIE model CDF/010 tray dryer at 50 °C to reduce its viscosity.

For the transesterification of both biodiesels, an automated batch reactor, Didatec model RQ-DT-135/EL, was used. Animal fats (chicken fat and pork fat) were used as raw material, methanol was used as solvent and a sodium hydroxide (NaOH) catalyst, which were homogenized, forming sodium methoxide (CH3O-Na+). The presence of a catalyst is necessary to increase the reaction rate and yield of the transesterification process. In the industry the main catalysts used are alkaline catalysts (NaOH and KOH), thanks to the fact that they have very good solubility in methanol and their price is quite low in the market [9]. The reaction conditions were: 4 hours of duration, at a temperature of 56 ºC and an agitation speed of 450 rpm. The chemical reaction of transesterification is shown in Figure 2.1.

Figure 2.1 Chemical reaction of biodiesel transesterification

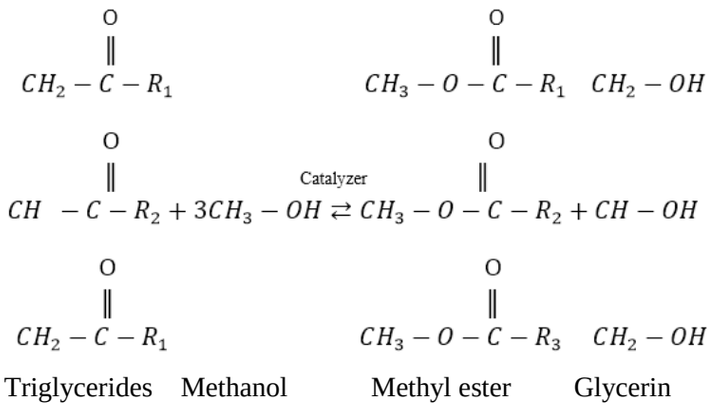

Source: (S. Rezania et al., 2019)

When the time of the reaction was finished, the mixture was extracted in 2 test tubes of 1000 ml and 2000 ml; leaving it to rest for 12 h; after which, and after settling the mixture, it was possible to differentiate the fatty acid methyl ester from the glycerin. Next, the fatty acid methyl ester and the glycerin were separated in different containers. Then, the fatty acid methyl ester was washed with distilled water using a 1000 ml separatory funnel to remove the remaining glycerol residues in the mixture. Two filtration methods were used to eliminate suspended solids; the first was gravimetric filtration with 11 µm Whatman paper and then with Purolite rigth 10 ion exchange resin. As mentioned above, biodiesel is a biofuel that is completely miscible with conventional diesel and its mixtures in any of its proportions have the possibility of improving the qualities of the fuel. The proportions used to prepare the diesel-biodiesel blends were: D-10, D-20, D-40, D-50, D-60, D-80, D-90. The nomenclature of the blends represents the percentage by mass of diesel and the remainder is the percentage by mass of biodiesel; for example, D-10 is defined as 10 percent diesel and 90 percent biodiesel. These blends were performed on an Ohasus brand digital pelletizing balance, with an uncertainty of ± 0.2 g.

2.2 Physicochemical análisis

The physicochemical properties of the diesel-biodiesel samples were determined in accordance with established standards and methods (ASTM D6751 and EN14214). The properties determined for the blends were: free acid number, copper strip corrosion at 40 °C and 100 °C, sulfated ash contents, flash point, density, specific gravity at 29.5 °C, density °API, specific weight, viscosity and freezing point. A detailed description of the procedure for obtaining each physicochemical property will be given below.

2.2.1 Free acid number

The acidity index was determined using method EN 14104 of Standard EN14214, which uses an alcoholic solution as titrant and phenolphthalein as color indicator. A method very similar to the one mentioned is the simple green visual method, which is the one used in this work to obtain the values of the acid number. The acid number is defined as the amount of milligrams of KOH or NaOH (mg) necessary to neutralize the free fatty acids present in one gram of oil or fat and is a measure of the degree of hydrolysis of a fat [10].

2.2.2 Flash point

The flash point is determined from the ASTM D-92 method, which is similar to the ASTM D-93 method of ASTM D6751. This method called "Cleveland open cup", defines the flash and ignition temperatures of all petroleum products, except those fuels that have an open cup flash temperature below 79°C and below 400°C. Approximately 70 ml of test sample is placed in a test vessel. The temperature of the vessel is rapidly increased by means of a burner and then the flame is controlled to generate a slower temperature rise steadily as the flash point is approached [11].

2.2.3 Density, specific gravity, API density and specific weight

These properties are determined using the ASTM D 1298 method of ASTM 6751. The method describes how to perform the analyses of density, specific gravity, API density and specific gravity. At present, density meters are reliable and efficient equipment to obtain the analyses described above. For this reason, the Anton Paar DMA 4100M density meter was used to analyze these properties.

2.2.4 Kinematic viscosity at 40 °C

The kinematic viscosity was specified according to ASTM D 445 of ASTM D 6751. Kinematic viscosity can be measured based on the time measurement of a known volume of sample flowing under gravity, passing through a calibrated glass capillary tube (viscometer) at ambient conditions [12]. Also, kinematic viscosity is related to dynamic viscosity through density. Having the value of the dynamic viscosity, the kinematic viscosity of a fluid can be calculated, observe the following Equation (Eq.1):

$$\boldsymbol{v} = \frac{\boldsymbol{\mu}}{\boldsymbol{\rho}} \tag{1}$$

where:
v: kinematic viscosity
μ*:* dynamic viscosity
ρ: density

The results of the kinematic viscosity analysis for each mixture were obtained from Eq. 1, where the dynamic viscosity is analyzed with the Anton Paar Physica MCR 101 rheometer and the density with the Anton Paar DMA 4100M density meter.

2.2.5 Freezing point

The freezing point is determined using the ASTM D 97 method of the ASTM D 6751 standard, for which a wide-mouth container is taken and ice and salt are placed inside. Then, test tubes with biodiesel and diesel-biodiesel blends are placed in the container. When the formation of solids (ice) begins in the biodiesel and the blends inside the tubes, the temperature is measured and this will be the freezing point value of that fuel [13].

2.3 Raman Spectroscopy

Raman spectroscopy is an analytical technique in the near-infrared range, based on the phenomenon of inelastic molecular vibration/rotation that causes frequency changes due to energy exchange with matter through the collision of molecules [14]. Samples of diesel-biodiesel blends were analyzed in quintuplicate using a QE65000 Raman spectrometer (Ocean Optics, Edinburgh, UK) equipped with a symmetrical cross Czerny-Turner optical bench, 101 mm focal length, an RPB 785 fiber optic test and a Hamamatsu S7031-1006 detector with a spectral range between 780 and 940 nm. The spectrometer was operated with SPECTRA SUIT software (version 2.0.162, Ocean Optics, Edinburgh, UK) to establish the interface between the computer and the Raman equipment. To perform the analysis of the samples, 30 mL of each mixture was deposited in an amber glass vial and subsequently a laser beam was applied at 785 nm with a power of 20 mW for 10 s. All Raman spectra were collected in the range of -81 to 2104 cm-1 at 25 ◦C. Data between 0-99 cm-1 and 1902-2104 cm-1 were omitted because they had higher spectral noise. Therefore, the spectral data between 100 and 1901 cm-1 were used.

2.4 Development of chemometric models,

For the development of the chemometric models, an experimental database was created, where the absorbances of the Raman spectra of the blends of both biodiesels (matrix X) and the results of the physicochemical properties (vector Y) were used. Microsoft Excel 2013 (Microsoft, Redmond, WA, USA) was used to create the matrices. Matrix X consisted with a composition of 850 wavelength values and 18 samples between of the diesel-biodiesel blends (15 300 absorbance samples) and matrix Y had for each physicochemical property one column and 18 samples in the rows. Subsequently, the X matrix was exported to Quasar v1.7.0 software to initially pre-process the data for a better fit.

The dimensionality of the data was then reduced using principal component analysis (PCA). The first step of the pretreatment was to minimize noise and spectral errors of the chemometric models, developed by mathematical and statistical treatments: auto-scaling and centering. Also, a first order derivative and the standard variable normalizations (SNV) and minimum-maximum (min-max) were used to achieve a greater correction of the spectrum; thus, obtaining an X-matrix transformation of 740 wavelength values and 18 samples. In the PCA, 740 wavelengths were reduced to 8 CP components with an explained variance of 97 %. For the construction, training and evaluation of the chemometric models, MATLAB numerical software was used in conjunction with its artificial neural network (ANN) Toolbox computational package (Demuth and Beale, 2021). For the predictability of the developed models, ANN employed back-propagation learning, with the Levenberg-Marquardt supervision algorithm, which has proven to be one of the most prominent in weight and bias optimization [12]. The model was trained with 70 % of the data (12 samples) and 30 % of the remaining data (6 samples) was used for model testing and validation. The indicators or statistical criteria used for the accuracy of the chemometric models were the root mean square error (RMSE), mean absolute percentage error (MAPE) and the correlation coefficient (R2); and the paired data T-student's test was used to evaluate the reliability of the chemometric models. Figure 2.2 shows the schematic diagram of the development of the chemometric models.

Figure 2.2 Schematic diagram of the process of development and evaluation of chemometric models for the estimation of physicochemical properties

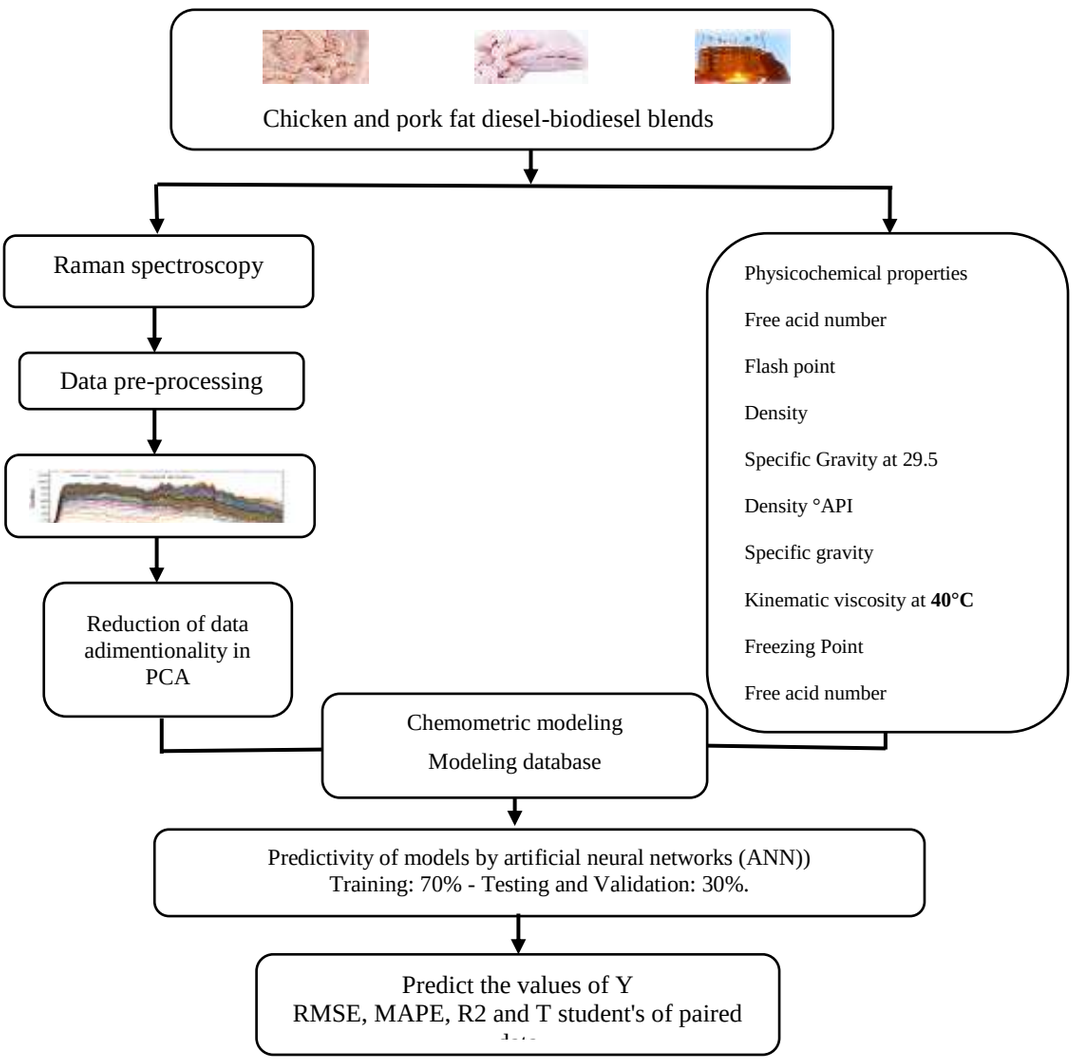

Source: Own Elaboration

3. Analysis and results

3.1 Interpretation of Raman Spectra

3.1.1 Raman spectra of chicken diesel-biodiesel blends of chicken fat.

Figure 3.1 shows that the Raman spectra obtained on the chicken fat diesel-biodiesel samples have spectral bands covering the following ranges: 260-542, 550-685, 685-711, 950-1100, 1180-1325, 1363-1447 and 1460-1750 cm-1:

The region between 260-542 cm-1 is related to the stretching and bending vibrations of C-O, C-C-O and C-C-C that form the molecular structure of fatty acid methyl ester [15].

The spectral region between 685-711 cm-1 is assigned to the stretching vibrations of C-O and C-C-O, and to the bending vibrations of O-C-O. On the other hand, the band between 711-950 cm-1 is a product of the C-C and C-H stretching vibrations present in the fatty acid methyl ester [16].

The region present between 950-1100 cm-1 is attributed to the bending vibrations of the C-H and C-O-H bonds of the fatty acid methyl ester [17].

The spectral region between 1180-1325 presents 2 peaks, these correspond to the stretching vibrations of the C-O, C-O-C bonds and the bending C-H and O-C-H vibrations [18].

The peak between 1363-1447 is due to the bending and oscillation vibrations of the C-H and O-H functional groups [18].

Figure 3.1 Absorbance bands present in chicken diesel-biodiesel blends

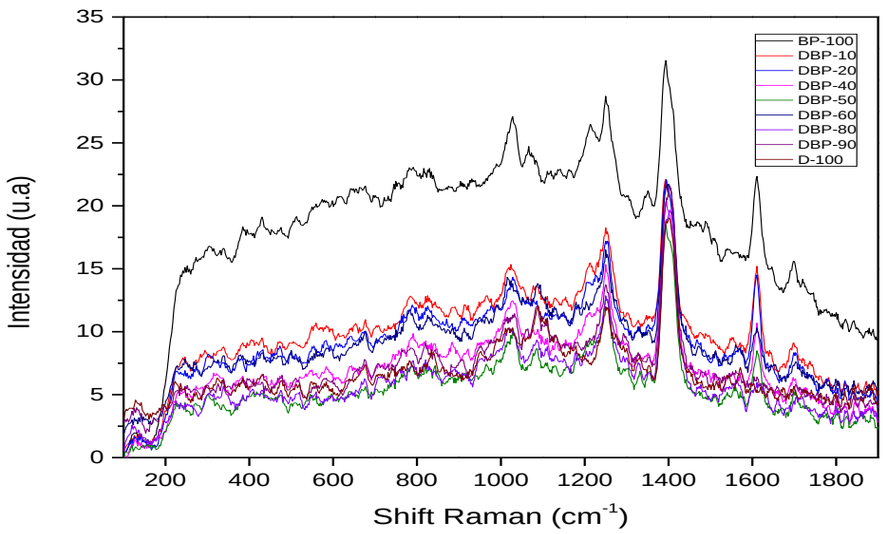

Source: Own Elaboration

Finally, the region between 1460-1750 are concerning the symmetric angular deformation of CH3, CeH, C=O axial deformation of aliphatics, saturated esters and asymmetric angular deformation in the CH2 plane, respectively [8].

3.1.1 Spectrum of pork fat diesel-biodiesel blends

Figure 3.2 corresponds to the Raman spectra of the pork fat diesel-biodiesel samples, these have spectral bands covering the ranges 750-900, 925-1140, 1186-1300, 1350-1460 and 1525-1740.

The region between 750 - 900 cm-1 is attributed to the C-C and CH stretching vibrations present in the fatty acid methyl ester [19].

Figure 3.2 Absorbance bands present in diesel-biodiesel blends of swine

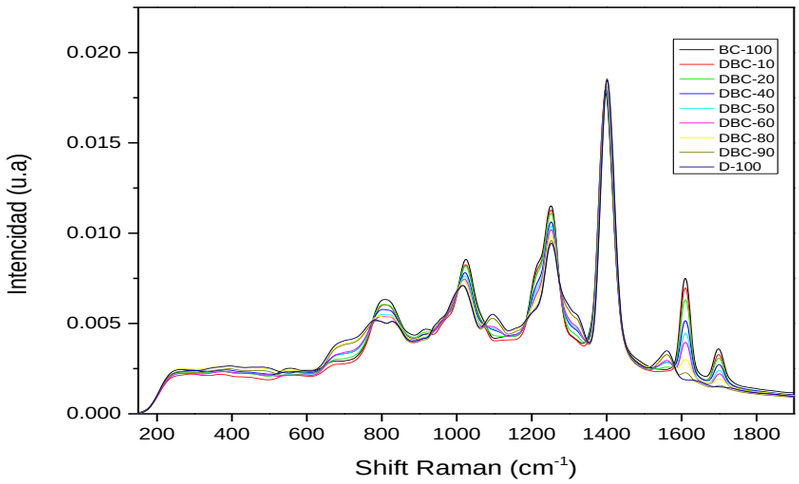

Source: Own Elaboration

The region between 925-1140 cm-1 these correspond to deformation vibrations in C-H and methylene (CH2) bonds, as well as COH bending vibrations identified in the bands 940-1074, bending vibrations of C-H and C-O-H bonds of esters, and to bending vibrations of C-N bonds of amino acids and proteins [17][18][20].

The spectral region between 1186-1300 cm-1corresponds to C-H and O-C-H vibrations, while the spectral bands 1350-1460 cm-1are due to bending and oscillation vibrations of C-H and O-H functional groups [18].

Finally, the spectral region between 1525-1740 cm-1 are due to the bending vibrations of the O-H functional group [21].

3.2 Physicochemical properties of chicken and pork fat biodiesels

The results of the conventional analyses of the physicochemical properties for the diesel-biodiesel blends are shown in Tables 3.1 and 3.2.

Table 3.1 Propiedades fisicoquímica del biodiesel de grasa de pollo y sus mezclas diésel-biodiesel

Mixtures	Acid number (mgKOH)	Flash point (°C)	Density (kg/m3)	Specific gravity 29.5°C	API density 15°C	Specific gravity	Viscosity (mm2/s)	Freezing point (°C)
$B-100$	0,340	162	878.0	0.8720	881.0	0.8800	3.35	4
$D-10$	0.310	144	871.5	0.8657	875.1	0.8731	3.27	1
$D-20$	0.280	132	865.0	0.8591	868.6	0.8665	2.69	-3
$D-40$	0.250	108	851.8	0.8459	855.5	0.8534	2.67	-5
$D-50$	0.200	100	846.0	0.8399	849.6	0.8475	2.38	-6
$D-60$	0.170	96	843.9	0.8379	847.6	0.8454	2.37	-7
$D-80$	0.140	90	829.0	0.8228	832.8	0.8305	1.70	-10
$D-90$	0.060	84	823.5	0.8172	827.2	0.8250	1.68	-12
$D-100$	0.056	78	816.9	0.8110	820.7	0.8180	1.54	-14

Source: Own Elaboration

Table 3.2 Physicochemical properties of pork fat biodiesel and its diesel-biodiesel blends

Mixtures	Acid number (mgKOH)	Flash point (°C)	Density (kg/m3)	Specific gravity 29.5°C	API density 15°C	Specific gravity	Viscosity (mm2/s)	Freezing point (°C)
$B-100$	0,310	160	870.0	0.8640	874.0	0.8720	3.67	11
$D-10$	0.250	142	868.6	0.8625	872.3	0.8702	3.49	8
$D-20$	0.220	124	862.2	0.8561	865.8	0.8637	3.19	6
$D-40$	0.200	108	850.3	0.8441	854.0	0.8518	2.70	3
$D-50$	0.170	100	843.1	0.8370	846.9	0.8447	2.42	1
$D-60$	0.140	96	838.7	0.8326	842.5	0.8403	2.35	-2
$D-80$	0.110	91	828.2	0.8220	832.0	0.8297	1.86	-7
$D-90$	0.080	82	821.2	0.8151	825.0	0.8227	1.76	-10
$D-100$	0.056	78	816.9	0.8110	820.7	0.8180	1.54	-14

Source: Own Elaboration

3.3 Chemometric models

3.3.1 Free Acid Number (InAc)

The InAc indicates the percentage (%) of free fatty acids in the biodiesel; this parameter corresponds to the amount of mg of KOH necessary for the neutralization of free fatty acids in one gram of fat [22]. It is very important to determine this property in the biofuel, since a high value of InAc can cause severe corrosion in internal combustion engine fuel systems [28]. The InAc obtained in chicken biodiesel (BP) and pig biodiesel (BC) were 0.34 mg KOH/g and 0.31 mg KOH/g respectively, these values are acceptable within the EN 14214 standard and were similar to [16]. For its part, the InAc of the BP had agreement with [23] [24][25], while the BC to [26] [27][28] [29][30][31].

To determine the chemometric models for each of the physicochemical properties, an analysis was made to know, with which; number of neurons would have a better fit. Five measurements were taken for each of the following neurons (n) 2, 4, 6, 8, 10 and 12, then the best of these was chosen, the selected measurements were compared and the one with the best prediction was determined. In the case of InAc the best prediction regression model was with 10n (see Table 3.3), its training (tr), validation (vl) and test (ts) statistical criteria were: R2tr=1.0000; R2vl=0.9937; R2ts=0.9975; MAPEtr=0.4194; MAPEvl=5.1968; MAPEts=2.2981; RMSEtr=0.0006; RMSEvl=0.0046 RMSEts=0.0040. The correlation coefficients between the actual and predicted values obtained in the 10n regression model, are observed in Figure 3.3, their results are: tr=0.99988, vl=0.99254, ts=0.99997 and yield (R)=0.99927. These results are superior to [32], [33] and similar to [34]

Table 3.3 Statistical criteria for chemometric models for InAc

Neurons	R^2tr	R^2vl	R^2ts	MAPEtr	MAPEvl	MAPEts	RMSEtr	RMSEvl	RMSEts
2	0.9946	0.9073	0.9633	4.9419	6.7808	6.9857	0.0069	0.0139	0.0166
4	0.9969	0.9300	0.9651	2.4173	3.7752	3.7997	0.0054	0.0093	0.0089
6	1.0000	0.9984	0.9878	0.0692	2.0431	5.6964	0.0001	0.0034	0.0089
8	0.9920	0.9949	0.9681	2.4082	1.6780	3.7489	0.0084	0.0041	0.0144
10	1.0000	0.9937	0.9975	0.4194	5.1968	2.2981	0.0006	0.0046	0.0040
12	1.0000	0.9923	0.9958	0.0066	2.8385	3.8166	0.0000	0.0061	0.0056

Source: Own Elaboration

Figure 3.3 Free acidity regression model, results of correlation coefficients: a) Training b) Validation c) Testing d) Performance

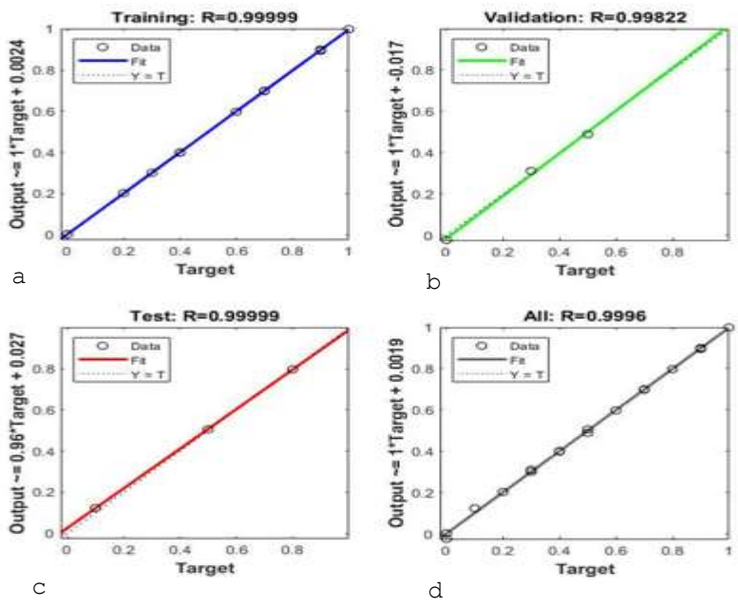

Source: Own Elaboration

3.3.2 Flash Point (PI)

One of the advantages of biodiesel over conventional diesel is that its IP is higher, which provides greater safety for handling, transportation and storage, thus reducing the risk of fire [23], [35]. According to Kirubakara *et al*. [23] mentions that after finishing the transesterification process, methanol should be removed from the final mixture to increase the flash point temperature. The results of the PI analysis for BP and BC were 162 ºC and 160 ºC, respectively, which are within the permissible parameters of ASTM D 6751. The BP result was similar to [25], while for BC it was similar to [36], [37]. In the case of PI the best fit model was with 4n (see Table 3.4), showing the following statistical indicators: R2tr=0.9999; R2vl=0.9994; R2ts=0.9876; MAPEtr=0.1013; MAPEvl=0.4491; MAPEts=0.7159; RMSEtr=0.2083; RMSEvl=0.6223; RMSEts=1.2099. Figure 3.4 shows the regression model obtained with 4n, where the correlation coefficients between the actual and predicted values were: Ent=0.99988, Val=0.99254, Pb=0.99997 and R=0.99927 respectively. The model results are superior to [18][32][4][4][38][33].

Table 3.4 Statistical criteria for chemometric models for the PI

Neuronas	R^2tr	R^2vl	R^2ts	MAPEtr	MAPEvl	MAPEts	RMSEtr	RMSEvl	RMSEts
2	0.9925	0.9956	0.9991	0.9946	0.5082	0.1864	2.1871	1.0343	0.3216
4	0.9999	0.9994	0.9876	0.1013	0.4491	0.7159	0.2083	0.6223	1.2099
6	0.9991	0.9970	0.9904	0.5382	0.6243	2.0388	0.8509	0.6759	2.2110
8	0.9992	0.9987	0.9953	0.6587	0.5638	1.2461	0.7888	0.6996	1.5200
10	0.9994	0.9728	0.9875	0.5187	2.6246	2.3487	0.6065	4.3206	3.0875
12	0.9999	0.9976	0.9940	0.1366	0.9302	0.8835	0.3281	1.0011	1.2195

Source: Own Elaboration

Figure 3.6 IP regression model, results of correlation coefficients: a) Training b) Validation c) Test d) Performance

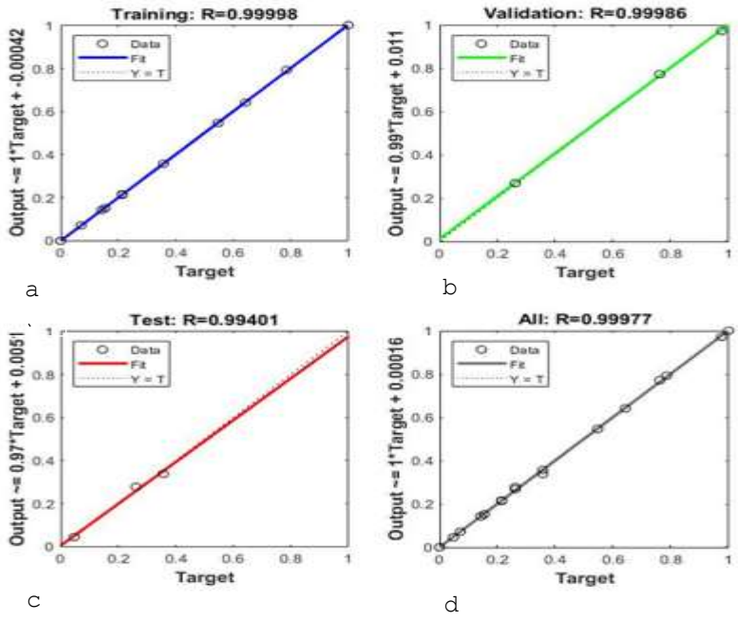

Source: Own Elaboration

3.3.3 Density, specific gravity 29.5 ºC (GE 29.5), API density (D API) and specific gravity (PE)

Density is a ratio expressed as mass per unit volume; it depends on the state of aggregation in which the substance is found and its temperature. Measuring density gives an idea of the mass content of the substance, being directly related to the energy of the fuel; the higher this value is, the better the profitability [39]. The density of biodiesel varies according to the nature of the raw material and influences the atomization efficiency [23]. The obtained values of specific gravity at 29.5 °C (GE 29.5), API density at 15°C (D API) and specific gravity (PE) are directly related to density. The density for BP and BC were 878 kg/m3 and 870 kg/m3 respectively, complying with EN 14214 standards and were similar to each other at [40][41].

Individually the density result of BP was similar to [35][42][39][23][43][44][45][46][47], while BC had agreement with [48][49][50][30]. The best fit chemometric model for density also, was with 4n (see Table 3.5), showing the following statistical criteria: R2tr=0.9985; R2vl=0.9721; R2ts=0.9972; MAPEtr=0.0512; MAPEvl=0.2060; MAPEts=0.1026; RMSEtr=0.7348; RMSEvl=1.9425; RMSEts=0.9753. Figure 3.5 shows the regression model obtained with 4n, where the correlation coefficients between the actual and predicted values were: Ent=0.99987, Val=0.99991, Pb=1 and R=0.99981. The values obtained in the model are higher than [18][32][32][51][38][33].

Table 3.5 Statistical criteria for density chemometric models.

Neuronas	R^2tr	R^2vl	R^2ts	MAPEtr	MAPEvl	MAPEts	RMSEtr	RMSEvl	RMSEts
2	0.9998	0.9998	0.9799	0.0268	0.0245	0.2610	0.3111	0.2315	2.4225
4	0.9985	0.9721	0.9972	0.0512	0.2060	0.1026	0.7348	1.9425	0.9753
6	0.9997	0.9934	0.9934	0.0293	0.1358	0.1550	0.3172	1.2116	1.5827
8	1.0000	0.9989	0.9714	0.0052	0.0662	0.2736	0.0562	0.6683	3.1331
10	0.9849	0.9341	0.9982	0.1963	0.3293	0.0863	2.2421	3.0298	0.8133
12	0.9999	0.9580	0.9951	0.0113	0.3012	0.1557	0.1456	4.0157	1.4155

Source: Own Elaboration

Figure 3.5 Density regression model, results of correlation coefficients: a) Training b) Validation c) Testing d) Performance

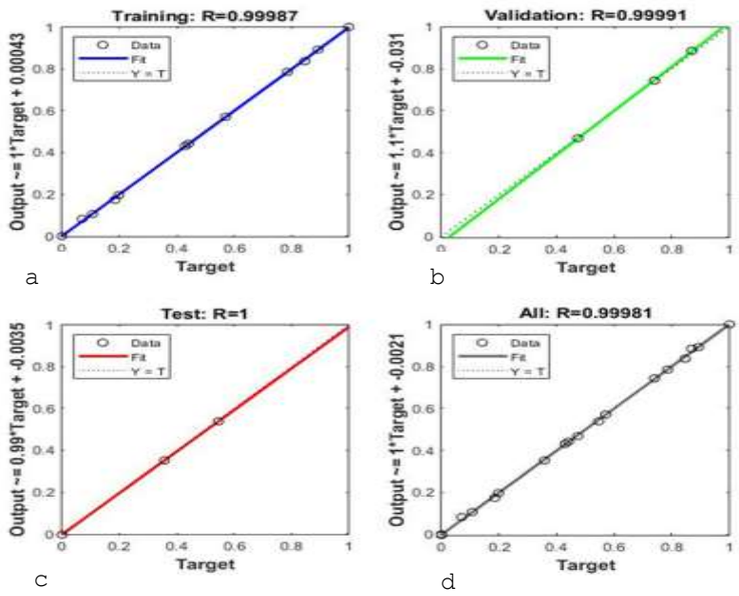

Source: Own Elaboration

The GE 29.5 results for BP and BC were 0.872 and 0.864, respectively. The chemometric model with the best fit was the 6n, reporting the following statistical criteria: R2tr=0.9997; R2vl=0.9988; R2ts=0.9943; MAPEtr=0.0245; MAPEvl=0.0550; MAPEts=0.1248; RMSEtr=0.0003; RMSEvl=0.0005; RMSEts=0.0012, see Table 3.6. The regression model obtained is shown in Figure 3.6, which shows the results of the correlation coefficients between the actual and predicted values of GE 29.5: Ent=0.99992, Val=0.99941, Pb=0.99930 and R=0.99963.

Table 3.6 Statistical criteria for chemometric models for GE 29.5 °C

Neuronas	R^2tr	R^2vl	R^2ts	MAPEtr	MAPEvl	MAPEts	RMSEtr	RMSEvl	RMSEts
2	0.9933	0.9965	0.9959	0.1030	0.1036	0.1123	0.0014	0.0009	0.0014
4	0.9998	0.9595	0.9522	0.0216	0.2234	0.1867	0.0003	0.0020	0.0024
6	0.9997	0.9988	0.9943	0.0245	0.0550	0.1248	0.0003	0.0005	0.0012
8	0.9999	0.9980	0.9504	0.0119	0.0932	0.6056	0.0001	0.0009	0.0055
10	0.9987	0.9986	0.9919	0.0466	0.0715	0.1828	0.0006	0.0007	0.0023
12	0.9964	0.9499	0.9911	0.0983	0.2807	0.1456	0.0012	0.0026	0.0017

Source: Own Elaboration

Figure 3.6 Regression model of GE 29.5, results of the correlation coefficients: a) Training b) Validation c) Testing d) Performance

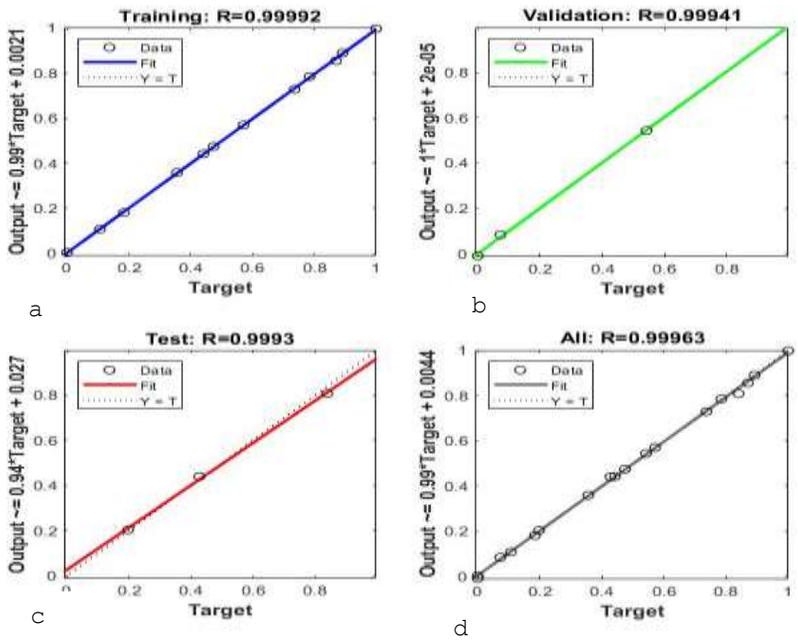

Source: Own Elaboration

The results of the analyses for D API for BP and BC were 881 ºAPI and 874 ºAPI respectively; the highest statistical criterion of the chemometric models was with 12n, with a fit of: R2tr=0.9997; R2vl=0.9964; R2ts=0.9994, MAPEtr=0.0238; MAPEvl=0.0587; MAPEts=0.0377; RMSEtr=0.3321; RMSEvl=0.6048; RMSEts=0.3361 (see Table 3.7). Figure 3.7 represents the regression model obtained for 12n, showing the results of the correlation coefficients between the actual and predicted values: Ent=0.99987, Val=0.99991, Pb=1 and R=0.99981.

Table 3.7 Statistical criteria of the chemometric models for D-API

Neuronas	R^2tr	R^2vl	R^2ts	MAPEtr	MAPEvl	MAPEts	RMSEtr	RMSEvl	RMSEts
2	1.0000	0.8523	0.9742	0.0046	0.2096	0.3322	0.0550	1.7900	3.0628
4	0.9858	0.9984	0.9603	0.0866	0.0662	0.1541	2.4164	0.6686	1.7198
6	1.0000	0.9901	0.9956	0.0001	0.0847	0.1286	0.0009	0.7845	1.5948
8	1.0000	0.9648	0.9992	0.0055	0.5066	0.0600	0.0538	5.0751	0.5385
10	1.0000	0.9956	0.9836	0.0042	0.1368	0.1414	0.0558	1.2156	1.6253
12	0.9997	0.9964	0.9994	0.0238	0.0587	0.0377	0.3321	0.6048	0.3361

Source: Own Elaboration

Figure 3.7 D-API regression model, results of correlation coefficients: a) Training b) Validation c) Testing d) Performance

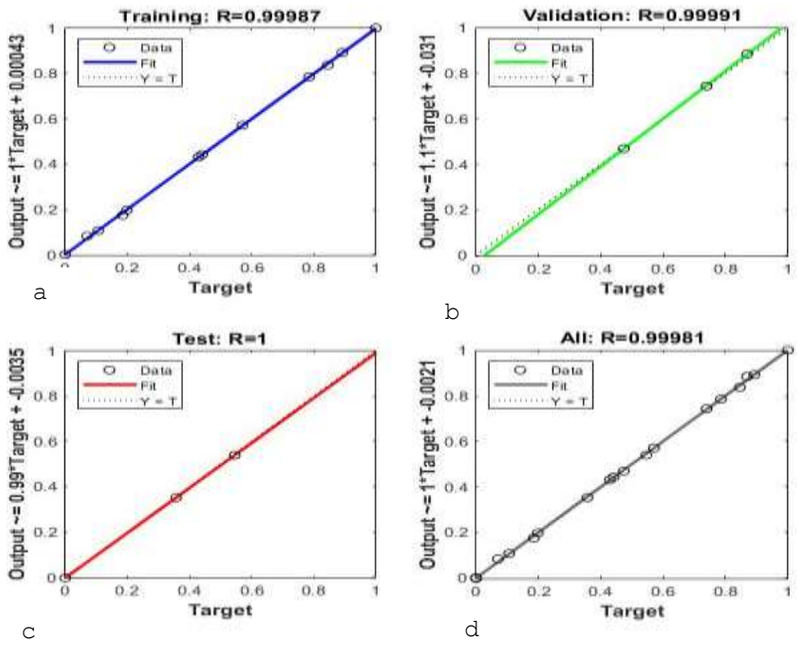

Source: Own Elaboration

The PE for BP and BC was 0.880 and 0.872 respectively; the chemometric model that showed the best statistical criteria was the 10n, with the following values: R2tr=0.9997; R2vl=0.9994; R2ts=0.9986, MAPEtr=0.0224; MAPEvl=0.0548; MAPEts=0.0773; RMSEtr=0.0003; RMSEvl=0.0005; RMSEts=0.0008 (see Table 3.8). The 10n regression model is depicted in Figure 3.8, where the correlation coefficients between the actual and predicted values are defined: Ent=0.99987, Val=0.99977, Pb=0.99943 and R=0.99973

Table 3.8 Statistical criteria of the chemometric models for PE.

Neuronas	R^2tr	R^2vl	R^2ts	MAPEtr	MAPEvl	MAPEts	RMSEtr	RMSEvl	RMSEts
2	0.9997	0.9821	0.9842	0.0311	0.1413	0.2671	0.0003	0.0013	0.0027
4	1.0000	0.9929	0.9867	0.0037	0.1157	0.2489	0.0000	0.0013	0.0023
6	0.9987	0.9813	0.9821	0.0662	0.1438	0.2618	0.0007	0.0017	0.0029
8	0.9979	0.9983	0.9658	0.0775	0.0408	0.4593	0.0009	0.0005	0.0045
10	0.9997	0.9994	0.9986	0.0224	0.0548	0.0773	0.0003	0.0005	0.0008
12	1.0000	0.9979	0.9877	0.0084	0.0904	0.1461	0.0001	0.0009	0.0015

Source: Own Elaboration

Figure 3.8 PE regression model, results of correlation coefficients: a) Training b) Validation c) Testing d) Performance

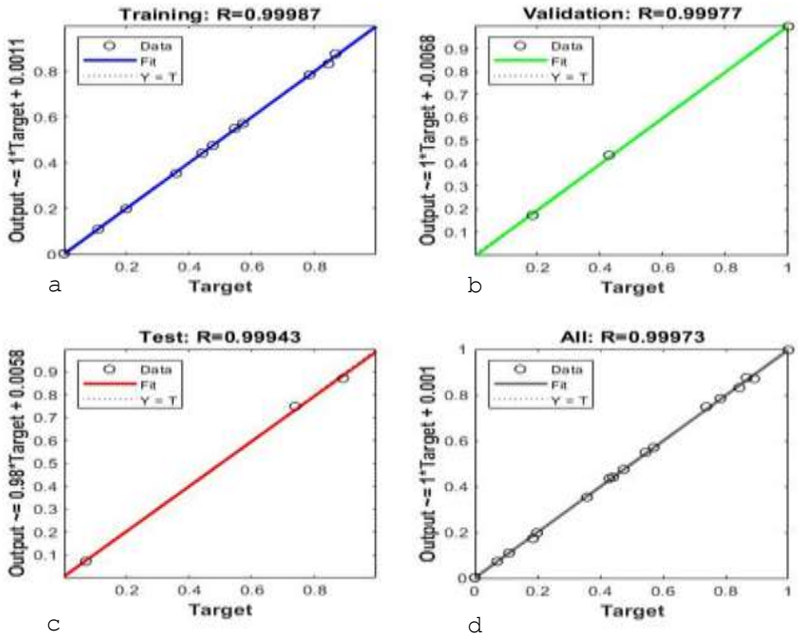

Source: Own Elaboration

3.3.4 Kinematic Viscosity at 40ºC (VCa40ºC)

The kinematic viscosity is one of the most important properties, since it affects the atomization of the fuel in the combustion chamber and, with it implies the formation of carbon residues in the engine [39]. The viscosity of biodiesel is mainly influenced by the experimental conditions and the magnitude of the transesterification reaction. Therefore, it is the main reason why fats and oils are transesterified to biodiesel, since this process significantly reduces this property [23]. The VCa40ºC of both biodiesel met the parameters of ASTM D 6751 and their values were 3.35 mm2/s and 3.67 mm2/s for both BP and BD. The VCa40ºC result for BP was similar to [24][44][23], while for BC it was [29][31]. For VCa40ºC the best fitting chemometric model was with 10n, which showed the following statistical prediction criteria: R2tr=0.9997; R2vl=0.9639; R2ts=0.9991, MAPEtr=0.2598; MAPEvl=3.2887; MAPEts=1.0709; RMSEtr=0.0109; RMSEvl=0.0635; RMSEts=0.0250 (see Table 3.9). Figure 3.9 shows the 10n regression model, numerically explaining the actual and predicted values of the correlation coefficients: Ent=0.99988, Val=0.99254, Pb=0.99997 and R=0.99927. The model values are higher than [18] [32] [32] [52] [51] [51] [3] [27] and similar to [53].

Table 3.9 Statistical criteria of chemometric models for VCa40ºC.

Neuronas	R^2tr	R^2vl	R^2ts	MAPEtr	MAPEvl	MAPEts	RMSEtr	RMSEvl	RMSEts
2	0.9997	0.9989	0.9947	0.3259	0.9939	1.4828	0.0128	0.0232	0.0450
4	0.9985	0.9962	0.9972	0.8441	1.5894	1.3159	0.0244	0.0414	0.0428
6	0.9995	0.9825	0.9521	0.5016	1.3561	2.9474	0.0169	0.0423	0.0900
8	0.9994	0.9989	0.9915	0.4864	0.5917	2.5321	0.0161	0.0144	0.0538
10	0.9997	0.9639	0.9991	0.2598	3.2887	1.0709	0.0109	0.0635	0.0250
12	0.9993	0.9832	0.9983	0.4604	1.3628	1.5344	0.0160	0.0518	0.0400

Source: Own Elaboration

Figure 3.9 Regression model of VCa40ºC, results of the correlation coefficients: a) Training b) Validation c) Testing d) Performance

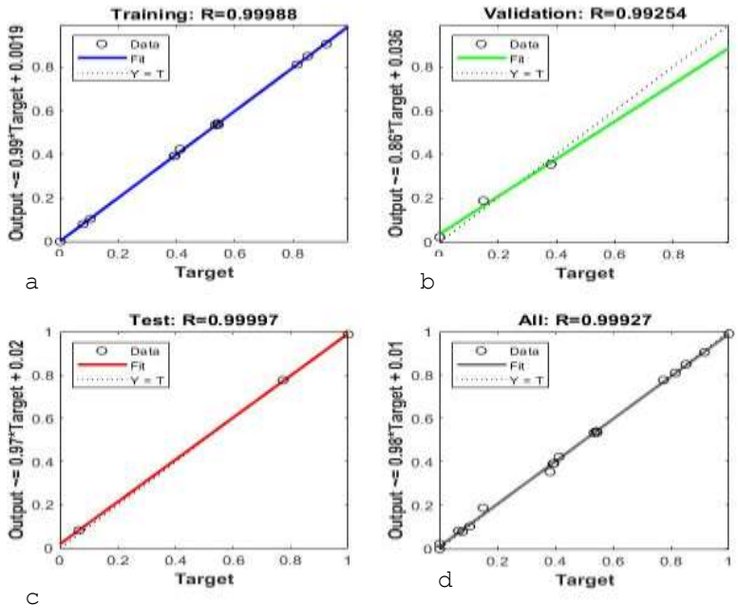

Source: Own Elaboration

3.3.5 Punto de congelación (PC)

The PC is the temperature at which a substance in a liquid state becomes a solid state [54]. At this point, the biofuel becomes semi-solid and loses the ability to flow freely. The impurities present without purification are the main cause that raise the pour point [23]. The PC for BP and BC were 4 ºC and 11 ºC, showing results of temperatures that are not favorable for the winter season [55]. The BP result agreed with [41][37] [46] while BC was similar to [36], [56].

The chemometric model that showed the highest accuracy for CP was de10n, with the statistical indicators: R2tr=0.9999; R2vl=0.9985; R2ts=0.9989, MAPEtr=-0.2702; MAPEvl=2.3893; MAPEts=0.5172; RMSEtr=0.0630; RMSEvl=0.2439; RMSEts=0.2131 (see Table 3.10). Figure 3.10 shows the correlation coefficients between the actual and predicted values of the regression model for 10n, showing the following results: Ent=0.99998, Val=0.99979, Pb=0.99996 and R=0.99986. The results of the PC model exceed [32][53].

Table 3.10 Statistical criteria for chemometric models for PC

Neuronas	R^2tr	R^2vl	R^2ts	MAPEtr	MAPEvl	MAPEts	RMSEtr	RMSEvl	RMSEts
2	0.9833	0.9985	0.9949	-1.7303	2.9711	-0.0051	0.7811	0.4158	0.3549
4	0.9979	0.9633	0.9748	6.6122	-17.877	-11.541	0.2924	1.0418	1.6706
6	0.9997	0.9971	0.9955	2.6554	-3.6504	-10.311	0.1250	0.4824	0.4660
8	0.9974	0.9993	0.9867	-1.5480	2.2415	5.8914	0.3541	0.2202	0.7317
10	0.9999	0.9985	0.9989	-0.2702	2.3893	0.5172	0.0630	0.2439	0.2131
12	0.9990	0.9974	0.9907	-0.7183	14.9598	20.9216	0.2201	0.3564	0.5797

Source: Own Elaboration

Figure 3.10 PC regression model, results of correlation coefficients: a) Training b) Validation c) Testing d) Performance

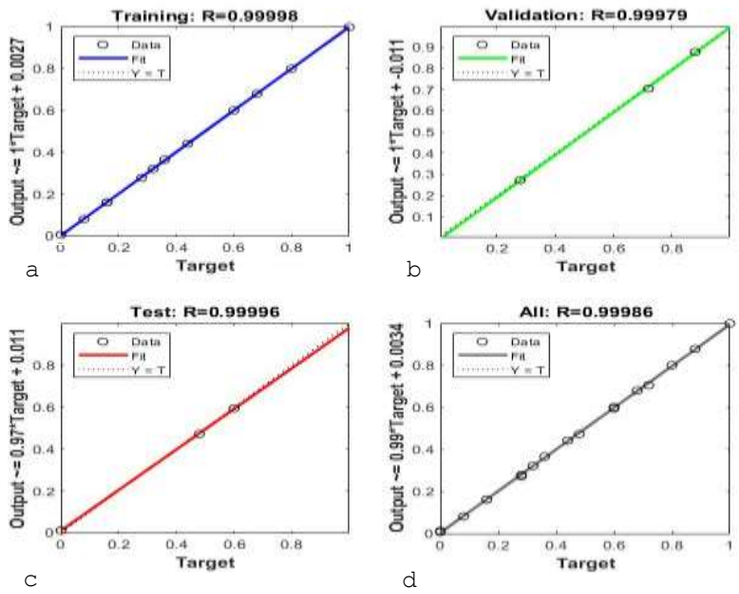

Source: Own Elaboration

3.3.6. Student's t-test on paired data

T-student's test is one of the most popular statistical techniques used to test whether the mean difference between two groups is statistically significant [57]. This test was used to evaluate the precision reliability of the results predicted by chemometric models and the results of physicochemical properties by conventional methods. T-student's distribution used the tailed test with a 95% confidence interval and with an external validation value of the T student's test (tv)= ± 2.11. Table 3.11 shows the confidence values of the T student's test (tc) for the physicochemical properties compared to the tv.

Table 3.11 T-student's paired data t-test results for physicochemical properties

Property	tv	tc	-tv > tc > tv
Free acid number	±2.11	1.40	Complied with
Flash point	±2.11	0.60	Complied with
Density	±2.11	0.30	Complied with
Specific gravity 29.5 ºC	±2.11	-0.92	Complied with
API density	±2.11	-1.10	Complied with
Specific gravity	±2.11	0.30	Complied with
Kinematic viscosity	±2.11	0.42	Complied with
Freezing point	±2.11	-0.42	Complied with

Source: Own Elaboration

In the definition of this test, we found that the tc results for all physicochemical properties are within the confidence interval of ±2.11, which is that there are no significant differences between the experimental data obtained by ASTM D6751 and EN 14214 and those predicted by the chemometric models. Therefore, with the paired data T-student's test it is demonstrated that the chemometric models have a predictive capacity to determine the values of the physicochemical properties as reliable as the analyses performed by conventional methods indicated by ASTM D6751 and EN 14214.

Conclusions

From the results obtained in this work, the following conclusions can be drawn:

The values of the physical and chemical properties of the diesel-biodiesel blends (D-10, D-20, D-40, D-50, D-60, D-80 and D-90) were within the range of values established in the ASTM D 6751 and EN 14214 standards.

The chemometric models built by means of neural networks from Raman spectroscopy information, allowed predicting: density, specific weight, API density, flash point, freezing point, kinematic viscosity of diesel/biodiesel blends with a precision and certainty similar to the standard methods established in the American and European norms.

The chemometric models obtained in this work allow determining: density, specific gravity, API density, flash point, freezing point, kinematic viscosity of diesel/biodiesel blends, requiring less working time. In addition, by not using reagents, they are more environmentally friendly.

The paired data T-student test was another useful statistical tool to determine the predictive ability of the chemometric models. The T-student confidence values (tc) for each model were within the range of external validation ($tv = \pm 2.11$).

Acknowledgment

I thank God and the saints for giving me the spiritual strength to complete these two years of studies in the master's program.

To Conacyt for the scholarship granted to finance my master's studies and research.

To my advisors and teachers, especially Dr. Mohamed for giving me the opportunity and confidence to come from abroad to study in the Master of Materials and Energy Engineering.

To my family for their loving and unconditional support that motivates me to keep going forward every day.

To all of you thank you very much.

Funding

This work has been funded by CONACYT [grant number 1165367].

References

[1] L. Al-Ghussain, "Global warming: review on driving forces and mitigation," *Environmental Progress and Sustainable Energy*, vol. 38, no. 1. John Wiley and Sons Inc., pp. 13–21, Jan. 01, 2019. doi:10.1002/ep.13041. https://aiche.onlinelibrary.wiley.com/doi/10.1002/ep.13041.

[2] M. A. El-Sharkawy, "Global warming: Causes and impacts on agroecosystems productivity and food security with emphasis on cassava comparative advantage in the tropics/subtropics," *Photosynthetica*, vol. 52, no. 2, pp. 161–178, 2014, doi: 10.1007/s11099-014-0028-7. https://link.springer.com/article/10.1007/s11099-014-0028-7.

[3] K. R. Bukkarapu and A. Krishnasamy, "A critical review on available models to predict engine fuel properties of biodiesel," *Renewable and Sustainable Energy Reviews*, vol. 155, p. 111925, Mar. 2022, doi: 10.1016/j.rser.2021.111925. https://www.sciencegate.app/document/10.1016/j.rser.2021.111925.

[4] K. R. Bukkarapu and A. Krishnasamy, "Predicting engine fuel properties of biodiesel and biodiesel-diesel blends using spectroscopy based approach," *Fuel Processing Technology*, vol. 228, Jun. 2022, doi: 10.1016/j.fuproc.2022.107227 https://www.sciencegate.app/document/10.1016/j.rser.2021.111925.

[5] S. Sayyed, R. K. Das, and K. Kulkarni, “Performance assessment of multiple biodiesel blended diesel engine and NOx modeling using ANN,” *Case Studies in Thermal Engineering*, vol. 28, Dec. 2021, doi: 10.1016/j.csite.2021.101509. https://www.sciencedirect.com/science/article/pii/S2214157X21006729.

[6] R. L. Naylor and M. M. Higgins, “The rise in global biodiesel production: Implications for food security,” *Global Food Security*, vol. 16. Elsevier B.V., pp. 75–84, Mar. 01, 2018. doi: 10.1016/j.gfs.2017.10.004. https://www.sciencedirect.com/journal/global-food-security/vol/12/suppl/C.

[7] H. M. Khan *et al.*, “Production and utilization aspects of waste cooking oil based biodiesel in Pakistan,” *Alexandria Engineering Journal*, vol. 60, no. 6, pp. 5831–5849, Dec. 2021, doi: 10.1016/j.aej.2021.04.043. https://www.sciencedirect.com/journal/alexandria-engineering-journal/vol/61/issue/10.

[8] International Energy Agency, “Renewable Energy Market Update - June 2023,” Paris, Jun. 2023. Accessed: Aug. 21, 2023. [Online]. Available: https://www.iea.org/reports/renewable-energy-market-update-june-2023. https://www.iea.org/reports/renewable-energy-market-update-june-2023.

[9] S. Rezania *et al.*, “Review on transesterification of non-edible sources for biodiesel production with a focus on economic aspects, fuel properties and by-product applications,” *Energy Conversion and Management*, vol. 201. Elsevier Ltd, Dec. 01, 2019. doi: 10.1016/j.enconman.2019.112155. https://www.sciencedirect.com/science/article/abs/pii/S0196890419311616.

[10] J. A. Aricetti and M. Tubino, “A green and simple visual method for the determination of the acid-number of biodiesel,” *Fuel*, vol. 95, pp. 659–661, May 2012, doi: 10.1016/j.fuel.2011.10.058. https://www.sciencedirect.com/journal/fuel/vol/96/suppl/C.

[11] S. K. Tulashie and F. Kotoka, “The potential of castor, palm kernel, and coconut oils as biolubricant base oil via chemical modification and formulation,” *Thermal Science and Engineering Progress*, vol. 16, May 2020, doi: 10.1016/j.tsep.2020.100480. https://www.sciencedirect.com/journal/thermal-science-and-engineering-progress/vol/19/suppl/C.

[12] A. T. Hoang, “Prediction of the density and viscosity of biodiesel and the influence of biodiesel properties on a diesel engine fuel supply system,” *Journal of Marine Engineering & Technology*, vol. 20, no. 5, pp. 299–311, Oct. 2021, doi: 10.1080/20464177.2018.1532734. https://www.tandfonline.com/doi/full/10.1080/20464177.2018.1532734.

[13] S. Banik *et al.*, “Production of biodiesel from neem seed oil,” *Bangladesh Journal of Scientific and Industrial Research*, vol. 53, no. 3, pp. 211–218, Sep. 2018, doi: 10.3329/bjsir.v53i3.38268. https://doaj.org/toc/2224-7157.

[14] G. W. Auner *et al.*, “Applications of Raman spectroscopy in cancer diagnosis,” *Cancer and Metastasis Reviews*, vol. 37, no. 4, pp. 691–717, Dec. 2018, doi: 10.1007/s10555-018-9770-9. https://pubmed.ncbi.nlm.nih.gov/30569241/.

[15] H. E. Tahir *et al.*, “Rapid prediction of phenolic compounds and antioxidant activity of Sudanese honey using Raman and Fourier transform infrared (FT-IR) spectroscopy,” *Food Chem*, vol. 226, pp. 202–211, Jul. 2017, doi: 10.1016/j.foodchem.2017.01.024. https://www.sciencedirect.com/journal/food-chemistry.

[16] S. Li, Y. Shan, X. Zhu, X. Zhang, and G. Ling, “Detection of honey adulteration by high fructose corn syrup and maltose syrup using Raman spectroscopy,” *Journal of Food Composition and Analysis*, vol. 28, no. 1, pp. 69–74, Nov. 2012, doi: 10.1016/j.jfca.2012.07.006. https://www.sciencedirect.com/journal/journal-of-food-composition-and-analysis

[17] S. P. Kek, N. L. Chin, Y. A. Yusof, S. W. Tan, and L. S. Chua, “Classification of entomological origin of honey based on its physicochemical and antioxidant properties,” *Int J Food Prop*, vol. 20, no. sup3, pp. S2723–S2738, Dec. 2017, doi: 10.1080/10942912.2017.1359185. https://www.sciencedirect.com/journal/journal-of-food-composition-and-analysis.

[18] A. Belay, W. K. Solomon, G. Bultossa, N. Adgaba, and S. Melaku, "Physicochemical properties of the Harenna forest honey, Bale, Ethiopia," *Food Chem*, vol. 141, no. 4, pp. 3386–3392, Dec. 2013, doi: 10.1016/j.foodchem.2013.06.035. https://www.sciencedirect.com/search?qs=Physicochemical%20properties%20of%20the%20Harenna%20forest%20honey%2C%20Bale%2C%20Ethiopia.

[19] F. Anguebes-Franseschi *et al.*, "Raman spectroscopy and chemometric modeling to predict physical-chemical honey properties from campeche, Mexico," *Molecules*, vol. 24, no. 22, Nov. 2019, doi: 10.3390/molecules24224091. https://www.mdpi.com/1420-3049/24/22/4091.

[20] M. Oroian and S. Ropciuc, "Romanian honey authentication using voltammetric electronic tongue. Correlation of voltammetric data with physico-chemical parameters and phenolic compounds," *Comput Electron Agric*, vol. 157, pp. 371–379, Feb. 2019, doi: 10.1016/j.compag.2019.01.008. https://dl.acm.org/doi/10.1016/j.compag.2019.01.008.

[21] A. D. V. Máquina, B. V. Sitoe, J. E. Buiatte, D. Q. Santos, and W. B. Neto, "Quantification and classification of cotton biodiesel content in diesel blends, using mid-infrared spectroscopy and chemometric methods," *Fuel*, vol. 237, pp. 373–379, Feb. 2019, doi: 10.1016/j.fuel.2018.10.011. https://www.sciencedirect.com/journal/fuel/vol/218/suppl/C.

[22] O. Aboelazayem, M. Gadalla, and B. Saha, "Derivatisation-free characterisation and supercritical conversion of free fatty acids into biodiesel from high acid value waste cooking oil," *Renew Energy*, vol. 143, pp. 77–90, Dec. 2019, doi: 10.1016/j.renene.2019.04.106. https://www.sciencedirect.com/journal/renewable-energy/vol/142/suppl/C

[23] M. Kirubakaran and V. Arul Mozhi Selvan, "A comprehensive review of low cost biodiesel production from waste chicken fat," *Renewable and Sustainable Energy Reviews*, vol. 82, pp. 390–401, Feb. 2018, doi: 10.1016/j.rser.2017.09.039. https://www.sciencedirect.com/journal/renewable-energy/vol/142/suppl/C.

[24] E. Fayyazi, B. Ghobadian, G. Najafi, and B. Hosseinzadeh, "An ultrasound-assisted system for the optimization of biodiesel production from chicken fat oil using a genetic algorithm and response surface methodology," *Ultrason Sonochem*, pp. 313–320, Mar. 2015, doi: http://dx.doi.org/10.1016/j.ultsonch.2015.03.007. https://www.sciencedirect.com/science/article/abs/pii/S1350417715000693

[25] K. Srinivasa Rao AssoProf, M. Engineering, and B. S. K Sundara Siva Rao Professor, "Experimental Studies on the Characteristics of Diesel Engine with Chicken Fat Methyl Ester," 2013. [Online]. Available: https://www.researchgate.net/publication/236864493. https://www.researchgate.net/publication/236864493_Experimental_Studies_on_the_Characteristics_of_Diesel_Engine_with_Chicken_Fat_Methyl_Ester.

[26] J. M. Dias, M. C. M. Alvim-Ferraz, M. F. Almeida, J. D. Méndez Díaz, M. Sánchez Polo, and J. Rivera Utrilla, "Biodiesel production using calcium manganese oxide as catalyst and different raw materials," *Energy Convers Manag*, vol. 65, pp. 647–653, Jan. 2013, doi: 10.1016/j.enconman.2012.09.016. https://www.sciencedirect.com/science/article/abs/pii/S0196890412003664.

[27] C. B. Ezekannagha, C. N. Ude, and O. D. Onukwuli, "Optimization of the methanolysis of lard oil in the production of biodiesel with response surface methodology," *Egyptian Journal of Petroleum*, vol. 26, no. 4, pp. 1001–1011, Dec. 2017, doi: 10.1016/j.ejpe.2016.12.004. https://www.sciencedirect.com/science/article/pii/S1110062116301556.

[28] N. Joy, J. Jayaraman, A. Mariadhas, P. Appavu, R. Tiwari, and R. Sarkar, "Effect of EGR on performance and emission of CI engine using biodiesel blend of pork lard," in *AIP Conference Proceedings*, American Institute of Physics Inc., Dec. 2020. doi: 10.1063/5.0034496. https://pubs.aip.org/aip/pof/search-results?page

[29] I. Ambat, V. Srivastava, S. Iftekhar, E. Haapaniemi, and M. Sillanpää, "Effect of different co-solvents on biodiesel production from various low-cost feedstocks using Sr–Al double oxides," *Renew Energy*, vol. 146, pp. 2158–2169, Feb. 2020, doi: 10.1016/j.renene.2019.08.061. https://www.sciencedirect.com/science/article/abs/pii/S0960148119312492.

[30] R. U. Azike and W. A. Raji, "Optimization of Biodiesel Production from Pig Lard using Sodium Hydroxide as Catalyst," *Nigerian Research Journal of Engineering and Environmental Sciences*, pp. 529–534, 2019, Accessed: Dec. 14, 2022. [Online]. Available: https://www.researchgate.net/profile/Wuraola.

[31] I. J. Stojković, M. R. Miladinović, O. S. Stamenković, I. B. Banković-Ilić, D. S. Povrenović, and V. B. Veljković, "Biodiesel production by methanolysis of waste lard from piglet roasting over quicklime," *Fuel*, vol. 182, pp. 454–466, Oct. 2016, doi: 10.1016/j.fuel.2016.06.014. https://www.sciencedirect.com/science/article/abs/pii/S0016236116304665.

[32] M. Agarwal, K. Singh, and S. P. Chaurasia, "Prediction of Biodiesel Properties from Fatty Acid Composition using Linear Regression and ANN Techniques," *Indian Chemical Engineer*, vol. 52, no. 4, pp. 347–361, Dec. 2010, doi: 10.1080/00194506.2010.616325. https://www.researchgate.net/search/publication.

[33] Gómez Rodríguez Karla Aída, "Estimación de propiedades del diésel y su uso en la determinación de un índice de calidad," Centro de Investigación Científica de Yucatán. AC, Mérida,Yucatán,2021.Accessed:May,13,2023.[Online].Available:https://cicy.repositorioinstitucional.mx/jspui/bitstream/1003/2120/1/PCER_M_Tesis_2021_Karla_Aida_Gomez_Rodriguez.pdf.

[34] M. Rajendra, P. C. Jena, and H. Raheman, "Prediction of optimized pretreatment process parameters for biodiesel production using ANN and GA," *Fuel*, vol. 88, no. 5, pp. 868–875, May 2009, doi: 10.1016/j.fuel.2008.12.008.
https://www.sciencedirect.com/science/article/abs/pii/S0016236108005024.

[35] I. B. Banković-Ilić, I. J. Stojković, O. S. Stamenković, V. B. Veljkovic, and Y.-T. Hung, "Waste animal fats as feedstocks for biodiesel production," *Renewable and Sustainable Energy Reviews*, vol. 32, pp. 238–254, Apr. 2014, doi: 10.1016/j.rser.2014.01.038. https://www.sciencedirect.com/science/article/abs/pii/S1364032114000495

[36] B. R. Moser, "Biodiesel production, properties, and feedstocks," *In Vitro Cellular and Developmental Biology - Plant*, vol. 45, no. 3. pp. 229–266, Jun. 2009. doi: 10.1007/s11627-009-9204-z. https://link.springer.com/article/10.1007/s11627-009-9204-z.

[37] V. T. Wyatt, M. A. Hess, R. O. Dunn, T. A. Foglia, M. J. Haas, and W. N. Marmer, "Fuel properties and nitrogen oxide emission levels of biodiesel produced from animal fats," *J Am Oil Chem Soc*, vol. 82, no. 8, pp. 585–591, Aug. 2005, doi: 10.1007/s11746-005-1113-2. https://link.springer.com/article/10.1007/s11746-005-1113-2

[38] M. I. Jahirul *et al.*, "Investigation of correlation between chemical composition and properties of biodiesel using principal component analysis (PCA) and artificial neural network (ANN)," *Renew Energy*, vol. 168, pp. 632–646, May 2021, doi: 10.1016/j.renene.2020.12.078. https://link.springer.com/article/10.1007/s11746-005-1113-2.

[39] R. Behçet, H. Oktay, A. Çakmak, and H. Aydin, "Comparison of exhaust emissions of biodiesel–diesel fuel blends produced from animal fats," *Renewable and Sustainable Energy Reviews*, vol. 46, pp. 157–165, Jun. 2015, doi: 10.1016/j.rser.2015.02.015.

[40] F. Toldrá-Reig, L. Mora, and F. Toldrá, "Trends in Biodiesel Production from Animal Fat Waste," *Applied Sciences*, vol. 10, no. 10, p. 3644, May 2020, doi: 10.3390/app10103644. https://www.sciencedirect.com/science/article/abs/pii/S1364032115001033.

[41] M. Keihani, H. Esmaeili, and P. Rouhi, “Biodiesel Production from Chicken Fat Using Nano-calcium Oxide Catalyst and Improving the Fuel Properties via Blending with Diesel,” *Biodiesel Production from Chicken Fat Using Nano-calcium Oxide Catalyst and Improving the Fuel Properties via Blending with Diesel*, pp. 522–529, May 2018, doi: DOI:10.22036/pcr.2018.114565.1453. https://www.researchgate.net/publication/325360075_Biodiesel_Production_from_Chicken_Fat_Using_Nano-calcium_Oxide_Catalyst_and_Improving_the_Fuel_Properties_via_Blending_with_Diesel.

[42] M. N. Mohiddin, A. A. Saleh, A. N. R. Reddy, and S. Hamdan, “A Study on Chicken Fat as an Alternative Feedstock: Biodiesel Production, Fuel Characterisation, and Diesel Engine Performance Analysis,” *International Journal of Automotive and Mechanical Engineering*, vol. 15, no. 3, pp. 5535–5546, Oct. 2018, doi: 10.15282/ijame.15.3.2018.10.0425. https://www.researchgate.net/publication/328121172_A_Study_on_Chicken_Fat_as_an_Alternative_Feedstock_Biodiesel_Production_Fuel_Characterisation_and_Diesel_Engine_Performance_Analysis.

[43] T. M. Mata, N. Cardoso, M. Ornelas, S. Neves, and N. S. Caetano, “Sustainable production of biodiesel from tallow, lard and poultry fat and its quality evaluation,” in *Chemical Engineering Transactions*, Italian Association of Chemical Engineering - AIDIC, 2010, pp. 13–18. doi: 10.3303/CET1019003. https://www.cetjournal.it/index.php/cet/article/view/8349.

[44] A. B. Fadhil, I. K. Saeed, L. I. Saeed, and M. H. Altamer, “Co-solvent ethanolysis of chicken waste: Optimization of parameters and characterization of biodiesel,” *Energy Sources, Part A: Recovery, Utilization, and Environmental Effects*, vol. 38, no. 19, pp. 2883–2890, Oct. 2016, doi: 10.1080/15567036.2015.1065299. https://www.tandfonline.com/doi/abs/10.1080/15567036.2015.1065299?journalCode=ueso20.

[45] V. Hariram *et al.*, “Biodiesel Extraction from Chicken Fat and Its Effect on the Performance and Emission Characteristics of the Diesel Engine,” *Nature Environment and Pollution Technology*, vol. 20, no. 4, Dec. 2021, doi: 10.46488/NEPT.2021.v20i04.041. https://www.researchgate.net/publication/356857545_Biodiesel_Extraction_from_Chicken_Fat_and_Its_Effect_on_the_Performance_and_Emission_Characteristics_of_the_Diesel_Engine

[46] Ramos, Dias, Puna, Gomes, and Bordado, “Biodiesel Production Processes and Sustainable Raw Materials,” *Energies (Basel)*, vol. 12, no. 23, p. 4408, Nov. 2019, doi: 10.3390/en12234408. https://www.mdpi.com/1996-1073/12/23/4408.

[47] N. Kinnal, G. Sujaykumar, S. W. D’costa, and G. S. Girishkumar, “Investigation on Performance of Diesel Engine by Using Waste Chicken Fat Biodiesel,” *IOP Conf Ser Mater Sci Eng*, vol. 376, p. 012012, Jun. 2018, doi: 10.1088/1757-899X/376/1/012012. https://iopscience.iop.org/article/10.1088/1757-899X/376/1/012012/pdf.

[48] T. M. Mata, N. Cardoso, M. Ornelas, S. Neves, and N. S. Caetano, “Evaluation of Two Purification Methods of Biodiesel from Beef Tallow, Pork Lard, and Chicken Fat,” *Energy & Fuels*, vol. 25, no. 10, pp. 4756–4762, Oct. 2011, doi: 10.1021/ef2010207. https://pubs.acs.org/doi/full/10.1021/ef2010207?src=recsys.

[49] C. B. Ezekannagha, C. N. Ude, and O. D. Onukwuli, “Optimization of the methanolysis of lard oil in the production of biodiesel with response surface methodology,” *Egyptian Journal of Petroleum*, vol. 26, no. 4, pp. 1001–1011, Dec. 2017, doi: 10.1016/j.ejpe.2016.12.004. https://www.sciencedirect.com/science/article/pii/S1110062116301556.

[50] R. Foroutan, R. Mohammadi, and B. Ramavandi, “Waste glass catalyst for biodiesel production from waste chicken fat: Optimization by RSM and ANNs and toxicity assessment,” *Fuel*, vol. 291, p. 120151, May 2021, doi: 10.1016/j.fuel.2021.120151. https://www.sciencegate.app/document/10.1016/j.fuel.2021.120151#google_vignette.

[51] V. Kumbhar, A. Pandey, C. R. Sonawane, A. S. El-Shafay, H. Panchal, and A. J. Chamkha, “Statistical analysis on prediction of biodiesel properties from its fatty acid composition,” *Case Studies in Thermal Engineering*, vol. 30, p. 101775, Feb. 2022, doi:10.1016/j.csite.2022.101775. https://www.sciencegate.app/document/10.1016/j.csite.2022.101775

[52] X. Meng, M. Jia, and T. Wang, “Neural network prediction of biodiesel kinematic viscosity at 313K,” *Fuel*, vol. 121, pp. 133–140, Apr. 2014, doi: 10.1016/j.fuel.2013.12.029. https://www.sciencegate.app/document/10.1016/j.csite.2022.101775.

[53] M. Mostafaei, “Prediction of biodiesel fuel properties from its fatty acids composition using ANFIS approach,” *Fuel*, vol. 229, pp. 227–234, Oct. 2018, doi: 10.1016/j.fuel.2018.04.148. https://www.sciencedirect.com/science/article/abs/pii/S0016236118307841

[54] B. Su et al., “Effect of Pour Point Depressants Combined with Dispersants on the Cold Flow Properties of Biodiesel-Diesel Blends,” JAOCS, Journal of the American Oil Chemists’ Society, vol. 98, no. 2, pp. 163–172, Feb. 2021, doi.org/10.1002/aocs.12456, https://aocs.onlinelibrary.wiley.com/doi/abs/10.1002/aocs.12456.

[55] Md. E. Hoque, A. Singh, and Y. L. Chuan, “Biodiesel from low cost feedstocks: The effects of process parameters on the biodiesel yield,” *Biomass Bioenergy*, vol. 35, no. 4, pp. 1582–1587, Apr. 2011, doi: 10.1016/j.biombioe.2010.12.024. https://www.sciencedirect.com/science/article/abs/pii/S0961953410004824.

[56] R. O. Dunn, “Effects of minor constituents on cold flow properties and performance of biodiesel,” Progress in Energy and Combustion Science, vol. 35, no. 6. pp. 481–489, Dec. 2009. doi: 10.1016/j.pecs.2009.07.002.
https://www.sciencedirect.com/science/article/abs/pii/S0360128509000331.

[57] P. Mishra, U. Singh, C. Pandey, P. Mishra, and G. Pandey, “Application of student’s t-test, analysis of variance, and covariance,” *Ann Card Anaesth*, vol. 22, no. 4, p. 407, 2019, doi: 10.4103/aca.ACA_94_19. https://pubmed.ncbi.nlm.nih.gov/31621677/.